Int. J. Electrochem. Sci., 14 **(2019)** 4371 – 4382, doi: 10.20964/2019.05.62

International Journal of
ELECTROCHEMICAL
SCIENCE
www.electrochemsci.org

Synthesis and Electrochemical Performance of Polypyrrole/Graphene Nanocomposites for the Detection of Formaldehyde

Z. Y. Cai[1,2,], F. F. Lin[2], T. Wei[2], D. G. Fu[1], and L. Z. Pei[2]*

[1] State Key Laboratory of Bioelectronics, School of Chemistry and Chemical Engineering, Southeast University, Nanjing 210096, P. R. China
[2] Key Laboratory of Metallurgical Emission Reduction & Resources Recycling, Ministry of Education, School of Materials Science and Engineering, Anhui University of Technology, Ma'anshan, Anhui 243002, P. R. China
[*]E-mail: caizhengyu0555@163.com

Received: 5 February 2019 / *Accepted:* 12 March 2019 / *Published:* 10 April 2019

Polypyrrole/graphene nanocomposites have been synthesized via a simple *in-situ* pyrrole polymerization process. The polypyrrole/graphene nanocomposites were analyzed by X-ray diffraction (XRD), scanning electron microscopy (SEM), transmission electron microscopy (TEM), high-resolution TEM (HRTEM) and Fourier transform infrared spectroscopy (FTIR) spectra. The results show that the sphere-like polypyrrole particles with the size of less than 500 nm attach to the surface of the graphene nanosheet-shaped structures with the size of less than 10 μm. The polypyrrole/graphene nanocomposites modified glassy carbon electrode exhibits good electro-catalytic performance for formaldehyde in neutral solution. The nanocomposites modified glassy carbon electrode shows an irreversible current peak located at +0.2 V. The detection limit and linear detection range are 0.028 μM and 0.001–2 mM. The polypyrrole/graphene nanocomposites reveal great potential to detect formaldehyde in liquid environment.

Keywords: Graphene/polypyrrole nanocomposites, Glassy carbon electrode, Electrochemical performance, Formaldehyde.

1. INTRODUCTION

Formaldehyde is a kind of important environmental pollutant which can cause serious diseases, such as pulmonary edema, cancer and leukaemia, et al.[1-3] Formaldehyde is usually soluble in aqueous solution and widely used in liquid products, even liquid foods, bubble bath and human biological fluids containing formaldehyde [4-6]. The International Agency for Research on Cancer and World Health Organization defined the formaldehyde as the carcinogenic to human with the guideline

value of 29.97 μM [7,8]. To ensure the human health and environmental safety, it is essential to develop rapid, sensitive method for the trace of the formaldehyde concentration in aqueous solution.

Various methods for the detection of formaldehyde in different environments have been reported. High performance liquid chromatography [9-11], electrochemical detection method [12-14], spectrometry [15,16], gas chromatography [17], capillary electrophoresis [4], mass spectrometry [18] and chemiluminescence method [19] were reported for formaldehyde detection with different analytical performance. Among these methods, electrochemical detection method is favorable for the detection of formaldehyde in aqueous solution owing to simple measurement process, rapidity, high sensitivity and low cost. For example, Cheng et al. [12] developed a palladium nanowire arrays modified glassy carbon electrode as the detection unit of electrochemical sensor to detect formaldehyde. The nanowire arrays modified glassy carbon electrode showed the detection limit of 0.5 μM and linear detection relationship in the concentration range of 0.002–1 mM. Jin et al. [20] reported the dynamic reaction of formaldehyde on gold electrode in alkaline solution by *in-situ* time-resolved IR spectro-electrochemistry method. Pt-Pd nanoparticles and a Nafion-modified glassy carbon electrode was applied for the electrochemical detection of formaldehyde showing a detection limit of 3 μM and linear relationship between 10 μM to 1 mM [21]. However, the electrochemical detection performance including detection limit and linear detection range still need be further improved. The key factor for improving the electrochemical performance to detect formaldehyde is to select efficient electrode materials. Therefore, it is essential to explore novel and efficient electrode materials for the electrochemical detection of formaldehyde.

Graphene is a kind of important inorganic conducting electrode material showing good electro-catalytic performance due to good electron conductivity with π trajectory [22]. Graphene nanocomposites with conducting polymers can simultaneously maintain the performance of the graphene and polymers [23-27]. Polypyrrole was reported to be used as the typical polymer electrode materials owing to good electron conductivity and electrochemical properties [28]. For example, Hui et al. [29] reported the composites with flower-like cobalt nanostructures, polypyrrole and graphene oxide modified glassy carbon electrode for the electrochemical detection of nitrite. The electrochemical performance for the detection of nitrite had been improved owing to the synergistic effect between the polypyrrole/graphene oxide and flower-like cobalt nanostructures. Wang et al. [30] reported the nanocomposites composed of graphene oxide, polypyrrole and honeycomb-like cobalt nanostructures for the electrochemical detection performance of the glucose with a low detection limit of 29 nM and linear detection range of 0.5 μM to 2.667 mM. Fe_3O_4/polypyrrole/graphene oxide nanocomposites modified glassy carbon electrode showed good electrochemical sensing performance for the detection of hydrazine [31]. These stimulate us to research the electrochemical performance of the polypyrrole/graphene nanocomposites modified glassy carbon electrode for formaldehyde detection. Nanocomposites containing polypyrrole and graphene might generate the synergistic role enhancing the electrochemical detection performance of the sensors. However, to date, the synthesis and electrochemical detection performance of the polypyrrole/graphene nanocomposites are rarely reported.

In this paper, the polypyrrole/graphene nanocomposites have been obtained by a simple *in-situ* pyrrole polymerization process. The polypyrrole/graphene nanocomposites were analyzed by X-ray

diffraction (XRD), scanning electron microscopy (SEM), transmission electron microscopy (TEM), high-resolution TEM (HRTEM) and Fourier transform infrared spectroscopy (FTIR) spectra. The polypyrrole/graphene nanocomposites were used as the glassy carbon electrode modified materials for the electrochemical detection of formaldehyde in aqueous solution. The polypyrrole/graphene nanocomposites modified glassy carbon electrode showed great application potential in the sensors for the detection of formaldehyde.

2. EXPERIMENTAL PROCEDURE

Graphene (>99.5%, Alfa Aesar) was purchased from Carbon Materials Co., Ltd. of P. R. China. Pyrrole monomer (A. R. grade), N,N-dimethylformamide (A. R. grade), alcohol (A. R. grade), hydrogen chloride solution (A. R. grade) and polypyrrole (A. R. grade) were purchased from the Shanghai Aladdin Bio-Chem Technology Co., Ltd. of P. R. China. Formaldehyde solution (38%), ammonium peroxydisulfate (APS, A. R. grade), acetone (A. R. grade) and KCl (A. R. grade) were obtained from Sinopharm Chemical Reagent Co., Ltd. of P. R. China. Distilled water was used during the experimental process.

100 mg graphene was dispersed into 10 mL 1 M hydrogen chloride solution with the ultrasonic stirring for 30 min. And 0.1 mL pyrrole monomer was added into the hydrogen chloride solution with the graphene under continous ultrasonic stirring. Then 10 mL ammonium peroxydisulfate was also slowly added into the above solution with the continous ultrasonic stirring. The mixed hydrogen chloride solution with the graphene, pyrrole and ammonium peroxydisulfate was stirred and reacted for 5 h at room temperature. The obtained composite products were collected by the centrifugation. The precipitate was washed and extracted via the distilled water and acetone, respectively for several times.

The polypyrrole/graphene nanocomposites modified glassy carbon electrode was obtained by a casting process. Prior to the modification, the glassy carbon electrode (diameter of 3 mm) was polished with 0.05 μm alumina slurries repeatedly to obtain mirror-like surface and rinsed by distilled water and alcohol, respectively. The glassy carbon electrode was dried in the air. The polypyrrole/graphene nanocomposites were dispersed into the N,N-dimethylformamide solvent and sonicated for 1 h. Then 10 μL suspension with the polypyrrole/graphene nanocomposites was dropped onto the pre-polished mirror-like surface of the glassy carbon electrode and dried in the air under an infrared lamp.

XRD measurement of the nanocomposites was recorded on the X-ray diffraction system (Bruker AXS D8, Germany) with Cu Kα radiation (λ=1.5406 Å), scan rate of 0.05 °s^{-1} and 2θ in the range of 20°-80°. The morphology of the nanocomposites was analyzed by SEM (nova nanoSEM FEI 430, Tokyo, Japan). TEM and HRTEM images of the nanocomposites were observed with JEM-2100 transmission electron microscopy (JEOL, 200 kV, Japan). The chemical bonding of the nanocomposites was analyzed according to the FTIR spectra on a Nicolet6700 infrared spectrometer (Thermo Nicolet Corporation, U.S.A.). The electrochemical performance of the polypyrrole/graphene nanocomposites was analyzed by cyclic voltammograms using CHI604D Electrochemical Analyzer (Shanghai Chenhua Apparatus Company, P. R. China). The electrochemical measurement was

performed in a conventional three-electrode system with the polypyrrole/graphene nanocomposites modified glassy carbon electrode as the working electrode, platinum as the counter electrode and saturated calomel electrode as the reference electrode. The starting potential was -1.0 V and the direction was scanned from -1.0 V to +1.0 V. The modified electrode was cleaned by distilled water and alcohol, respectively between subsequent runs in order to obtain the repeatability. All electrochemical experiments were performed at room temperature.

3. RESULTS AND DISCUSSION

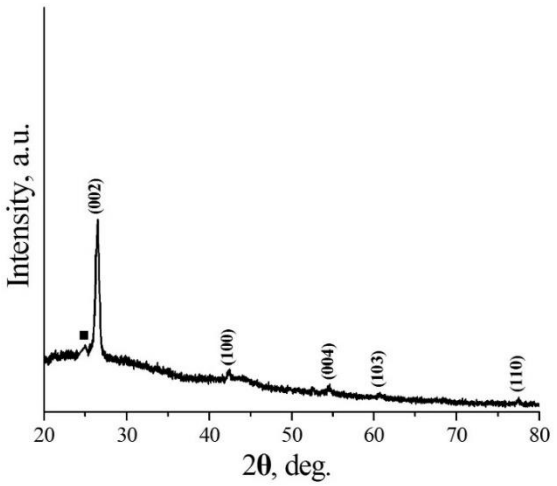

Figure 1. XRD pattern of the polypyrrole/graphene nanocomposites.

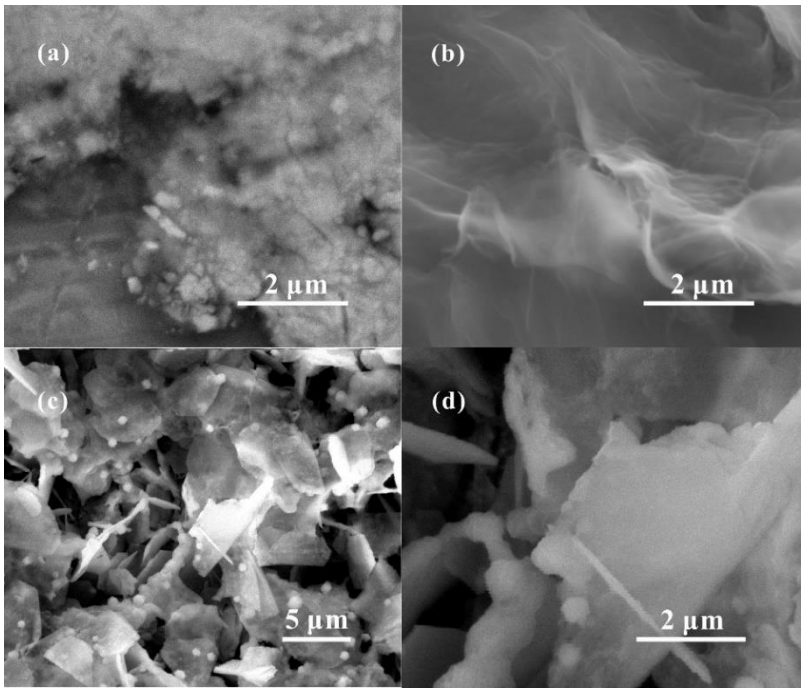

Figure 2. SEM images of the pyrrole, graphene and polypyrrole/graphene nanocomposites. (a) Pyrrole, (b) graphene, (c) and (d) polypyrrole/graphene nanocomposites.

The phase of the polypyrrole/graphene nanocomposites was analyzed by XRD measurement. Figure 1 shows the typical XRD pattern of the obtained nanocomposites. The diffraction peaks can be well indexed to hexagonal graphite-2H phase (JCPDS card, PDF 41-1487). Besides hexagonal graphite-2H phase, a wide peak at $2\theta = 25^{o}$ (designated by ■) exists in the XRD pattern which is caused by the polypyrrole [30]. The results show the formation of the polypyrrole and the polypyrrole/graphene nanocomposites are composed of hexagonal graphite and polypyrrole.

The morphologies of the raw materials pyrrole, graphene and polypyrrole/graphene nanocomposites were firstly observed and compared by SEM which is shown in Figure 2. It is observed that the dried pyrrole powder is composed of nanoscale sphere-like particles with the size of less than 200 nm (Figure 2a). The graphene shows the nanosheet-shaped structures with the folds and wrinkles (Figure 2b). The thickness of the graphene nanosheet-shaped structures is less than 50 nm. The SEM images of the polypyrrole/graphene nanocomposites show that the sphere-like polypyrrole particles attach to the surface of the graphene nanosheet-shaped structures (Figure 2c and 2d) indicating the formation of the polypyrrole/graphene nanocomposites. The size of the graphene nanosheet-shaped structures is less than 10 μm. The diameter of the sphere-like polypyrrole particles is less than 500 nm. The diameter of the sphere-like polypyrrole particles is larger than that of the raw material pyrrole which may originate from the polymerization of the pyrrole.

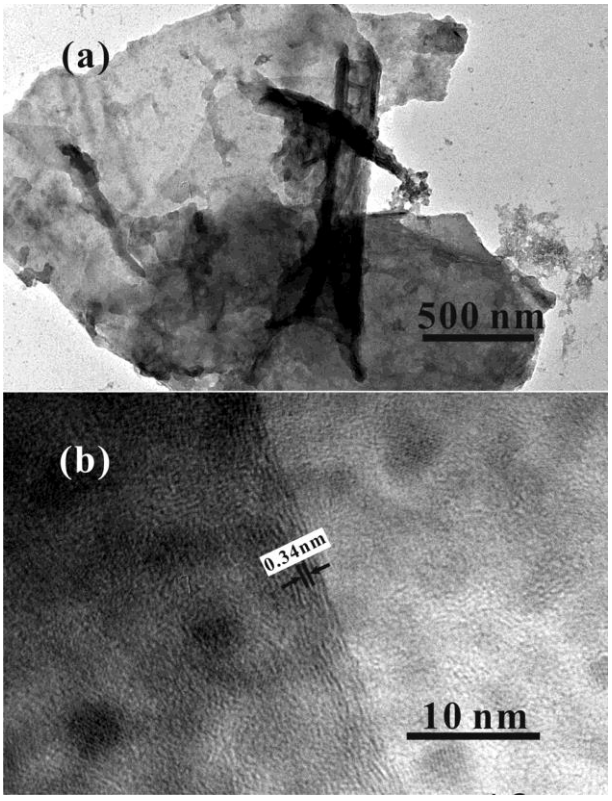

Figure 3. TEM and HRTEM images of the polypyrrole/graphene nanocomposites. (a) TEM, (b) HRTEM.

The morphology of the polypyrrole/graphene nanocomposites is further analyzed by TEM and HRTEM observation which is shown in Figure 3. The TEM image (Figure 3a) shows that the

nanocomposites have typical lamellar structures with the thickness of less than 50 nm. The nanoscale particles are distributed at the surface of the graphene nanosheet-shaped structure. The observed morphology is similar to that observed by SEM. HRTEM image (Figure 3b) reveals that the graphene has clear lattice fringes. The graphene has clear lattice fringes with the interplanar spacing of 0.34 nm which corresponds to the crystallographic plane of {002} of the graphene. The transmission electron microscopy images further confirm the formation of the polypyrrole/graphene nanocomposites.

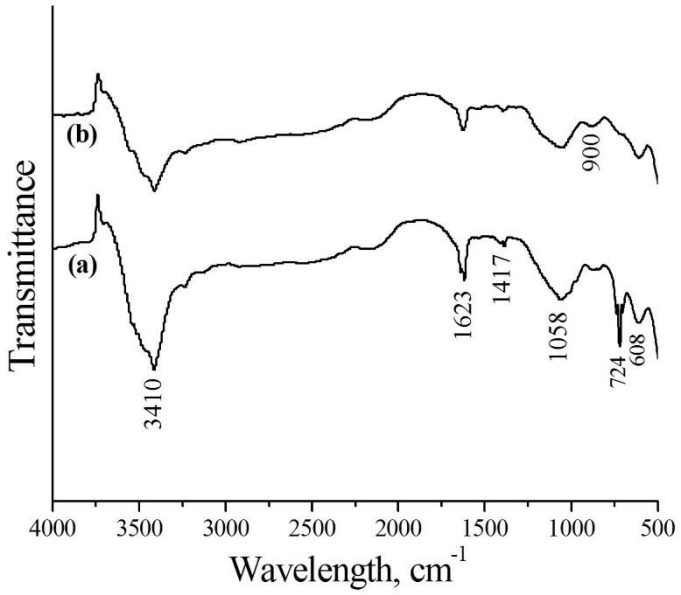

Figure 4. FTIR spectra of the polypyrrole and polypyrrole/graphene nanocomposites. (a) Polypyrrole, (b) polypyrrole/graphene nanocomposites.

Figure 4 represents the FTIR spectra of the polypyrrole and polypyrrole/graphene nanocomposites in the wavelength range of 4000–500 cm^{-1}. The absorption peaks located at 3410 cm^{-1} and 1417 cm^{-1} are associated with the N-H and C–N stretching vibration of the pyrrole ring [32]. The absorption peak at 1623 cm^{-1} corresponds to hydroxyl groups. The FTIR absorption peaks located at 1058 cm^{-1}, 900 cm^{-1}, 724 cm^{-1} and 608 cm^{-1} are ascribed to the C–O–C vibration in C–O–C (epoxy), the doping state of polypyrrole, C-H and =C–C [24,33,34]. It is obviously observed that the FTIR spectrum of the polypyrrole/graphene nanocomposites is similar to that of the polypyrrole. The vibrational spectra of the nanocomposites further confirm the polymerization of the polypyrrole followed by the formation of the nanocomposites which may originate from the hydrogen bonding and π-π interaction between the rings of the pyrrole.

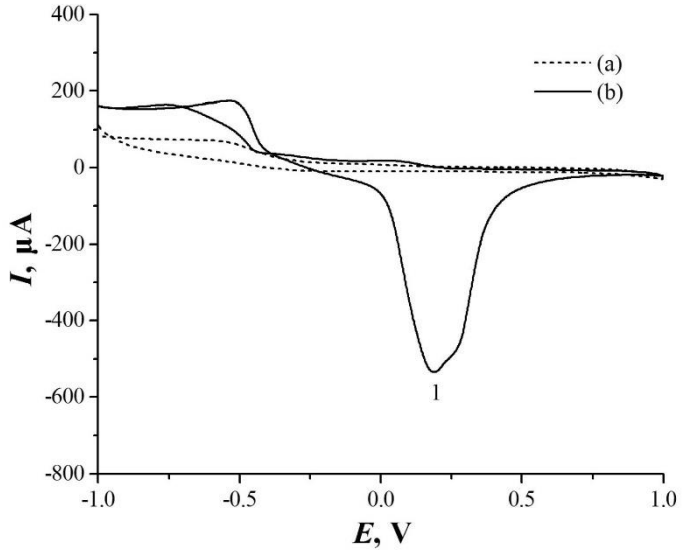

Figure 5. Cyclic voltammograms of the bare glassy carbon electrode, polypyrrole/graphene nanocomposites modified glassy carbon electrode in the presence of 2 mM formaldehyde with 0.1 M KCl. (a) Bare glassy carbon electrode, (b) polypyrrole/graphene nanocomposites modified glassy carbon electrode.

The electrochemical properties of the polypyrrole/graphene nanocomposites modified glassy carbon electrode were investigated by cyclic voltammetry method. The cyclic voltammograms (CVs) of 2 mM formaldehyde in 0.1 M KCl solution at the bare glassy carbon electrode, polypyrrole/graphene nanocomposites modified glassy carbon electrode are shown in Figure 5. There are no electrochemical CVs of 2 mM formaldehyde at the bare glassy carbon electrode (Figure 5a) suggesting that the bare glassy carbon electrode has no electro-catalytic role toward formaldehyde in KCl solution. The background current on the polypyrrole/graphene nanocomposites modified glassy carbon electrode is much larger than that on the bare glassy carbon electrode (Figure 5b) which may be caused by the larger surface area of the nanocomposites. The result is similar to that reported by other groups [35-38]. Observed from Figure 5b, the electrochemical process is characterized by an irreversible current peak. The irreversible current peak is located at +0.2 V. The oxidation peak located at +0.2 V corresponds to the oxidation of the formaldehyde on the polypyrrole/graphene nanocomposites modified glassy carbon electrode. In the presence of 0.1 M formaldehyde with 0.1 M sulfuric acid solution, the Pt-Pd nanoparticles and a Nafion-modified glassy carbon electrode showed an oxidation peak at +0.58 V [22]. The CV of 0.5 mM formaldehyde at the Os(byp)2-poly(vinylpyridine) (POs-EA) modified screen-printed electrode (SPE) showed a pair of oxidation and reduction peaks at +0.24 V and +0.30 V, respectively [39]. Compared with the above reports, the oxidation peak potential for formaldehyde is lower suggesting that the polypyrrole/graphene nanocomposites have superior electrochemical activity for formaldehyde. The good electro-catalytic activity at the polypyrrole/graphene nanocomposites modified glassy carbon electrode may be ascribed to fast electronic conductivity and good synergistic role between the polypyrrole and graphene. It was reported that the formaldehyde could be oxidized to carbon dioxide via the electro-oxidation process at various electrodes [35]. The polypyrrole/graphene nanocomposites modified glassy carbon electrode

has a low oxidation potential suggesting that the electrochemical oxidation process of the formaldehyde via a direct electrochemical oxidation pathway [12].

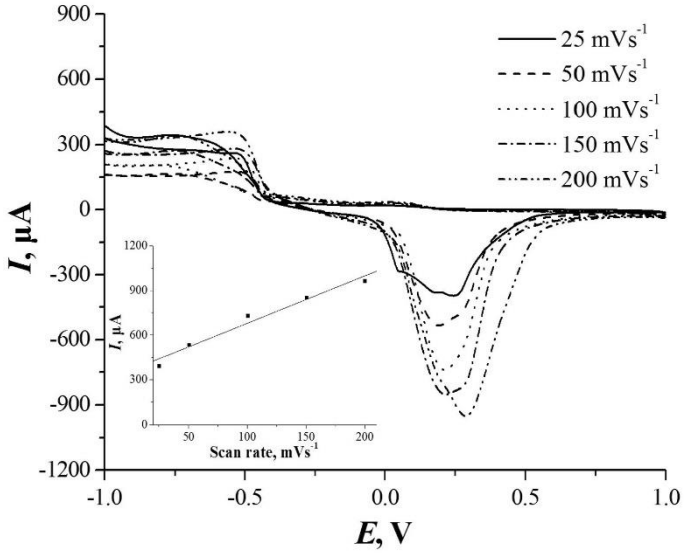

Figure 6. Cyclic voltammograms of the polypyrrole/graphene nanocomposites modified glassy carbon electrode in the presence of 2 mM formaldehyde with 0.1 M KCl using various scan rates. The inset in the bottom-left part is the plot between the peak current and scan rate.

To research the reaction kinetics of the formaldehyde oxidation, the polypyrrole/graphene nanocomposites modified glassy carbon electrode was scanned at different scan rates in 2 mM formaldehyde with 0.1 M KCl solution.

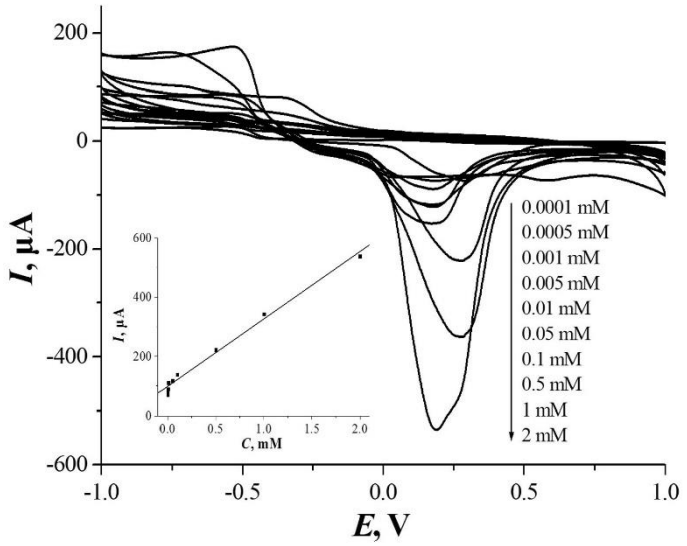

Figure 7. Cyclic voltammograms of the polypyrrole/graphene nanocomposites modified glassy carbon electrode in the presence of 0.1 M KCl solution containing formaldehyde with various concentrations. The inset in the bottom–left part is the plot curve between the peak current and formaldehyde concentration.

The electrochemical CVs are shown in Figure 6. As the increase of the scan rate, the peak current increases correspondingly. Moreover, the current of the cathodic peak and anodic peak increases obviously with an increase in the scan rate ranging from 25 $mV \cdot s^{-1}$ to 200 $mV \cdot s^{-1}$. The peak current is linearly proportional to the scan rate from 25 $mV \cdot s^{-1}$ to 200 $mV \cdot s^{-1}$ (inset in the bottom-left part of Figure 6). These results reveal that the electrochemical process of the formaldehyde at the polypyrrole/graphene nanocomposites modified glassy carbon electrode behaves as the typical adsorption controlled process [14,20,39].

The electrochemical responses of the polypyrrole/graphene nanocomposites modified glassy carbon electrode were measured with various concentrations of formaldehyde in 0.1 M KCl solution. Figure 7 shows the electrochemical cyclic voltammograms of formaldehyde with various concentrations at the nanocomposites modified glassy carbon electrode.

Table 1. Analytical data of formaldehyde using the polypyrrole/graphene nanocomposites modified glassy carbon electrode.

CV peak	Regression equation[a]	Correlation coefficient (R)	Linear range (mM)	Detection limit (μM)[b]	Sensitivity ($\mu A mM^{-1}$)
cvp1	I_p=98.746+225.427C	0.988	0.001-2	0.028	225.427

[a] Where I_p and C refer to the current (μA) of the CV peak and formaldehyde concentration (mM)
[b] The detection limit was calculated using S/N = 3

Table 2. Comparison of the detection parameters for formaldehyde at the polypyrrole/graphene nanocomposites modified glassy carbon electrode with reported literatures.

Electrodes	Linear range (mM)	Detection limit (μM)	Ref.
Pd nanowire arrays modified glassy carbon electrode	0.002-1	0.5	[12]
Mesoporous silica electrode	0.001-1	1.2	[13]
Pt NP/PANI/MWNCS modified glassy carbon electrode	0.001-1	0.046	[14]
Pt-Pd nanoparticles and a Nafion-modified glassy carbon electrode	0.01-1	3	[15]
Pd nanoparticles and TiO_2 modified glassy carbon electrode	0-17.7	15	[36]
Poly(GMA-*co*-MTM)FDH/Ppy composite film electrode	0.0033-0.1	0.15	[40]
Bio-functionalized $Si/SiO_2/Si_3N_4$ electrode	0.01-25	10	[41]
Polypyrrole/graphene nanocomposites modified glassy carbon electrode	0.001-2	0.028	Present work

The current of the oxidation peak increases with the concentration in the range from 0.0001–2 mM. The plot curve between the oxidation peak current and formaldehyde concentration reveals a linear relationship (inset in the bottom-left part of Figure 7). The detection limit is estimated by the

calculation using signal-noise ratio of 3 (S/N = 3). The analytical parameters of the formaldehyde at the polypyrrole/graphene nanocomposites modified glassy carbon electrode are listed in Table 1.

The detection limit is 0.028 μM. The linear detection range is 0.001–2 mM because range 0.0001-0.001 mM is out of 0.001-2 mM range. The correlation coefficient R and sensitivity are 0.988 and 225.427 μAmM^{-1}, respectively. Table 2 lists the comparison of the polypyrrole/graphene nanocomposites modified glassy carbon electrode with other electrodes. Comparing with the detection parameters of formaldehyde using other electrodes, the polypyrrole/graphene nanocomposites modified glassy carbon electrode has wide linear detection range and lower detection limit.

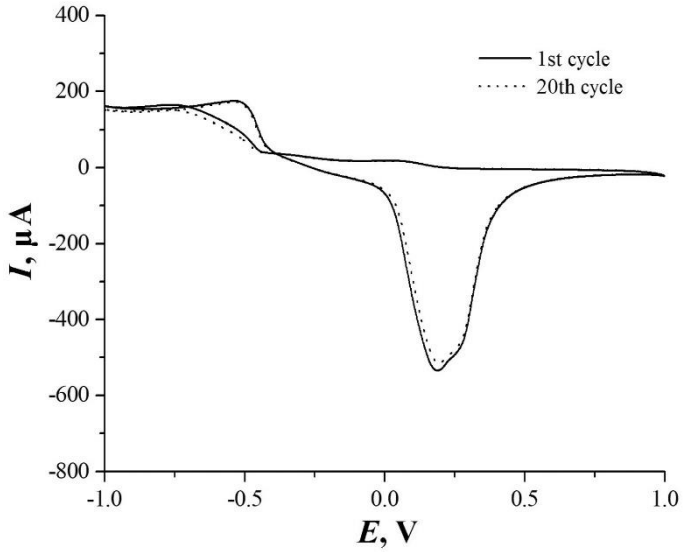

Figure 8. Cyclic voltammograms of the polypyrrole/graphene nanocomposites modified glassy carbon electrode in the presence of 2 mM formaldehyde with 0.1 M KCl recycling for the 1st and 20th time, respectively using the scan rate of 50 mVs^{-1}.

The repeatability and long term stability of the polypyrrole/graphene nanocomposites modified glassy carbon electrode are also analysed. Figure 8 shows the cyclic voltammograms of the nanocomposites modified glassy carbon electrode in the presence of 2 mM formaldehyde recycling for the 1st and 20th time, respectively. The relative standard deviation (R.S.D.) for the electrochemical response to 2 mM formaldehyde is 2.42% for twenty successive measurements. The long term stability is investigated by the storage of the polypyrrole/graphene nanocomposites modified glassy carbon electrode in ambient conditions for two weeks. The signal current shows a slight decrease after the modified electrode was stored for two weeks. The decrease of the signal current may be ascribed to the consumption of the formaldehyde [24].

4. CONCLUSIONS

In summary, polypyrrole/graphene nanocomposites have been synthesized via a simple *in-situ* pyrrole polymerization process. The sphere-like polypyrrole particles with the size of less than 500 nm

attach to the surface of the graphene nanosheet-shaped structures with the size of less than 10 μm. The electrochemical modified glassy carbon electrode is proposed based on the polypyrrole/graphene nanocomposites. The nanocomposites modified electrode exhibits good electro-catalytic performance for formaldehyde detection. The peak current is linearly proportional to the scan rate from 25 $mV \cdot s^{-1}$ to 200 $mV \cdot s^{-1}$ and formaldehyde concentration from 0.0001–2 mM. The detection limit and linear detection range are 0.028 μM and 0.001–2 mM, respectively. The polypyrrole/graphene nanocomposites exhibit great application potential for the electrochemical sensors to detect formaldehyde.

ACKNOWLEDGMENTS
This work was supported by the Natural Science Foundation of the Education Bureau of Anhui Province of China (KJ2017A057).

References

1. B. Y. Deng, Y. Liu, H. H. Yin, X. Ning, H. Lu, L. Ye and Q. X. Xu, *Talanta*, 91 (2012) 128.
2. P. F. Brandão, R. M. Ramos and J. A. Rodrigues, *Anal. Bioanal. Chem.*, 410 (2018) 6873.
3. A. Xu, Y. H. Tang and W. Y. Lin, *New J. Chem.*, 42 (2018) 8325.
4. X. Q. Zhao and Z. Q. Zhang, *Talanta*, 80 (2009) 242.
5. P. S. Spencer, *J. Neurol. Sci.*, 391 (2018) 141.
6. T. Y. Yang, K. K. Gu, C. B. Zhai, Q. Zhao, X. D. Yang and M. Z. Zhang, *New J. Chem.*, 42 (2018) 13612.
7. B. Peng, J. H. Zhang, C. H. Wu, S. Q. Li, Y. B. Li, H. X. Gao, R. H. Lu and W. F. Zhou, *J. Liq. Chromatogr. Relat. Technol.*, 37 (2014) 15.
8. S. D. Richardson, M. J. Plewa, E. D. Wagner, R. Schoeny and D. M. DeMarini, *Mutat. Res.*, 636 (2007) 178.
9. X. Xu, R. Su, X. Zhao, Z. Liu, D. Li, X. Y. Li, H. Q. Zhang and Z. M. Wang, *Talanta*, 85 (2011) 2632.
10. D. Wen, S. Guo, S. Dong and E. K. Wang, *Biosens. Bioelecron.*, 26 (2010) 1056.
11. J. Wang, P. Zhang, J. Q. Qi and P. J. Yao, *Sens. Actuat. B*, 136 (2009) 399.
12. Y. Zhang, M. Zhang, Z. Q. Cai, M. Q. Chen and F. L. Cheng, *Electrochim. Acta*, 68 (2012) 172.
13. T. Shimomura, T. Itoh, T. Sumiya, F. Mizukami and M. Ono, *Sens. Actuat. B*, 135 (2008) 268.
14. Y. Herschkovitz, I. Eshkenazi, C. E. Campbell and J. Rishpon, *J. Electroanal. Chem.*, 491 (2000) 182.
15. M. Zhang, F. L. Cheng, Z. Q. Cai and H. J. Yao, *Int. J. Electrochem. Sci.*, 5 (2010) 1026.
16. G. P. Jin, J. Li and X. Peng, *J. Appl. Electrochem.*, 39 (2009) 1889.
17. Q. F. Yi, W. Huang, X. Q. Liu, G. R. Xu, Z. H. Zhou and A. C. Chen, *J. Electroanal. Chem.*, 619 (2008) 197.
18. X. Cao, N. Wang, L. Wang, C. Mo, Y. J. Xu, X. L. Cai and G. Lin, *Sens. Actuat. B*, 147 (2010) 730.
19. J. W. Wang, P. Holt-Hindle, D. MacDonald, D. F. Thomas and A. Chen, *Electrochim. Acta*, 53 (2008) 6944.
20. R. W. Yan and B. K. Jin, *Chin. Chem. Lett.*, 24 (2013) 159.
21. Z. L. Zhou, T. F. Kang, Y. Zhang and S. Y. Cheng, *Microchim. Acta*, 164 (2009) 133.
22. J. P. Smith, J. P. Metters, D. K. Kampouris, C. Fernandez, O. B. Sutcliffe and C. E. Banks, *The Analyst*, 138 (2013) 6185.
23. S. Kruanetr, P. Pollard, C. Fernandez and R. Prabhu, *Int. J. Electrochem. Sci.*, 9 (2014) 5699.

24. Z. Rui, W. Huang, Y. Chen, K. X. Zhang, Y. Cao and J. C. Tu, *J. Appl. Polym. Sci.*, 134 (2017) 44840.
25. J. Li, Y. Zhang, H. Q. Xie, Y. Li and C. Zhen, *J. Solid State Electrochem.*, 21 (2017) 2201.
26. J. F. Duan, C. Zhu, Y. H. Du, Y. L. Wu, Z. Y. Chen, L. J. Li, H. L. Zhu and Z. Y. Zhu, *J. Mater. Sci.*, 52 (2017) 10470.
27. S. Y. Cao, C. S. Chen, X. D. Xi, B. Zeng, X. T. Ning, T. G. Liu, X. H. Chen, X. M. Meng and Y. Xiao, Vacuum, 102 (2014) 1.
28. M. G. Hosseini, H. Rasouli, E. Shahryai and L. Naji, *J. Appl. Polym. Sci.*, 134 (2017) 44926.
29. J. S. Wang and N. Hui, *Microchim. Acta*, 184 (2017) 2411.
30. N. Hui and J. S. Wang, *J. Electroanal. Chem.*, 798 (2017) 89.
31. Z. Y. Yang, Q. L. Sheng, S. Zhang, X. H. Zheng and J. B. Zheng, *Microchim. Acta*, 184 (2017) 2219.
32. Y. He, Y. Bai, X. Yang, J. Zhang, L. Kang, H. Xu, E. Shi, Z. Lei and Z. H. Liu, *J. Power Sources*, 317 (2016) 10.
33. Y. Zhao, J. Liu, Y. Hu, H. Cheng, C. Hu, C. Jiang, L. Jiang, A. Cao and L. Qu, *Adv. Mater.*, 25 (2013) 591.
34. K. V. Harpale, S. R. Bansode and M. A. More, *J. Appl. Polym. Sci.*, 134 (2017) 45170.
35. A. Safavi, N. Maleki, F. Farjami and E. Farjami, *J. Electroanal. Chem.*, 626 (2009) 75.
36. Q. F. Yi, F. J. Niu and W. Q. Yu, *Thin Solid Films*, 519 (2011) 3155.
37. C. S. Chen, W. W. Yu, T. G. Liu, S. Y. Cao and Y. H. Tsang, *Sol. Energ. Mat. Sol. C.*, 160 (2017) 43.
38. Z. Y. Chen, M. Xu, H. L. Zhu, T. Xie, W. H. Wang and Q. F. Zhao, *Appl. Surf. Sci.*, 286 (2013) 177.
39. W. W. Yu, X. A. Chen, W. Mei, C. S. Chen and Y. H. Tsang, *Appl. Surf. Sci.*, 400 (2017) 129.
40. S. K. Ozoner, E. Erhan, F. Yilmaz, P. Ergenekon and I. Anild, *J. Chem. Technol. Biotechnol.*, 88 (2013) 727.
41. M. B. Ali, M. Gonchar, G. Gayda, S. Paryzhak, M. A. Maaref, N. Jaffrezic-Renault and Y. Korpan, *Biosens. Bioelectron.*, 22 (2007) 2790.